Exploring the ability of chlorophyll *b* to bind to the CP43′ protein induced under iron deprivation in a mutant of *Synechocystis* PCC 6803 containing the *cao* gene

James Duncan[a], Thomas Bibby[a], Ayumi Tanaka[b], James Barber[a,*]

[a] *Wolfson Laboratories, Department of Biological Sciences, South Kensington Campus, Imperial College, London SW7 2AZ, UK*
[b] *Institute of Low Temperature Science, Hokkaido University, Sapporo 060-0819, Japan*

Received 11 February 2003; revised 21 March 2003; accepted 21 March 2003

First published online 3 April 2003

Edited by Stuart Ferguson

Abstract Cyanobacteria, unlike plants and green algae, do not contain chlorophyll (Chl) *b*. This is because of the absence of the *cao* gene which encodes the enzyme that catalyses a two step oxygenation of chlorophyllide *a* to chlorophyllide *b*. Recently, however, the *cao* gene of higher plants was engineered into *Synechocystis* PCC 6803 leading to Chl *b* synthesis in this cyanobacterium [Satoh et al., J. Biol. Chem. 276 (2001) 4293–4297]. Here we use this same *cao*-plus mutant to show that Chl *b* can bind to the CP43′ protein, expressed in cells exposed to low iron levels, which normally binds Chl *a* only. In so doing CP43′ is changed to a Chl *a*/Chl *b*-binding protein and in this respect resembles the closely related Chl *a*/Chl *b*-binding Pcb protein of prochlorophytes (green oxyphotobacteria). The results emphasise the possibility of using an in vitro system to elucidate factors which control the binding of these two different forms of chlorophylls to the six transmembrane helical light-harvesting proteins of oxygenic photosynthetic organisms.

Key words: *Synechocystis* PCC 6803; Photosystem II; *cao* gene

1. Introduction

Chlorophyll *b* (Chl *b*) is a ubiquitous accessory pigment in the chloroplasts of land plants and green algae and is bound to three transmembrane helical proteins encoded by *cab* genes [1]. According to the endosymbiotic theory [2], cyanobacteria are the ancestors of plant and algal chloroplasts [3] but paradoxically they do not contain Chl *b* but instead employ phycobiliproteins as accessory pigments [4]. The discovery, however, of a cyanobacterial-like organism which contained Chl *b* seemed to provide evidence for the missing link [5]. These Chl *b*-binding green oxyphotobacteria, known as prochlorophytes, like plants and green algae use this form of Chl to harvest light energy and transfer it to their reaction centres [6]. Surprisingly, gene sequencing showed that the Chl *b*-binding proteins of prochlorophytes are not encoded by *cab* genes but by *pcb* genes [7]. These genes encode six transmembrane helical proteins which are homologous with a cyanobacterial protein expressed only when the cells are exposed to low levels of iron. This protein, known as CP43′ because of its structural homology with the photosystem II (PSII) protein CP43 [8], is encoded by the iron-stress-induced *isi*A gene and, unlike the Pcb proteins, binds only Chl *a*. A possible reason for the difference between the CP43′ protein of cyanobacteria and Pcb proteins of prochlorophytes is that cyanobacteria lack the chlorophyll(ide) *a* oxygenase *cao* gene [9]. The enzyme encoded by this gene catalyses the conversion of chlorophyllide *a* to chlorophyllide *b* [9]. Recently the *cao* gene of higher plants has been engineered into cyanobacteria and its expression has resulted in the conversion of some Chl *a* to Chl *b* [10,11]. Here we explore the ability of the Pcb-like CP43′ protein to bind Chl *b* in a *cao*-plus mutant of the cyanobacterium *Synechocystis* PCC 6803 [10]. In so doing we are developing an experimental approach to gain a better understanding of the pigment-binding properties of the six transmembrane helical light-harvesting proteins which form a superfamily including the light-harvesting systems of PSII (CP43, CP47) and photosystem I (PSI) (N-terminal domain of PsaA and PsaB) reaction centres as well as the Pcb and CP43′ proteins [6,7].

2. Materials and methods

2.1. Growth conditions

Studies were conducted on CP43′-PSI and PSI preparations isolated from *Synechocystis* sp. PCC 6803 either having a histidine tag attached to the C-terminus of the PSII protein CP47 [12,13] or having the *cao* gene of *Arabidopsis thaliana* engineered into its genome [10]. Cells of both mutants were grown photoheterotrophically in mineral medium BG11 containing kanamycin (His-tagged mutant), chloramphenicol (*cao*-plus mutant) and glucose at 30°C and 70 μE/m^2/s illumination. Iron-stressed cultures were obtained by growing cells of either mutant in the same BG11 medium but lacking iron-containing compounds. Cultures were harvested after 3 days and in the case of iron-starved cultures, the cells had a characteristic blue shift in their long wavelength absorption band of about 8 nm compared with cells grown normally.

Thylakoid membranes were isolated using a procedure reported previously [12,13]. The isolated thylakoids (1 mg Chl/ml) were solubilised with 1% *n*-dodecyl β-D-maltoside (DM) at 4°C for 10 min and centrifuged at 45 000 rpm using a Beckman Ti70 rotor. In the case of the His-tagged mutant, the supernatant was passed through a Ni^{2+} affinity column resulting in the PSII fraction being bound to the

*Corresponding author. Fax: (44)-20-7594 5267.
E-mail address: j.barber@imperial.ac.uk (J. Barber).

Abbreviations: Chl, chlorophyll; DM, *n*-dodecyl β-D-maltoside; EM, electron microscopy; HPLC, high pressure liquid chromatography; PSII, photosystem II; PSI, photosystem I; SDS–PAGE, sodium dodecyl sulphate–polyacrylamide gel electrophoresis

0014-5793/03/$22.00 © 2003 Federation of European Biochemical Societies. Published by Elsevier Science B.V. All rights reserved.
doi:10.1016/S0014-5793(03)00323-5

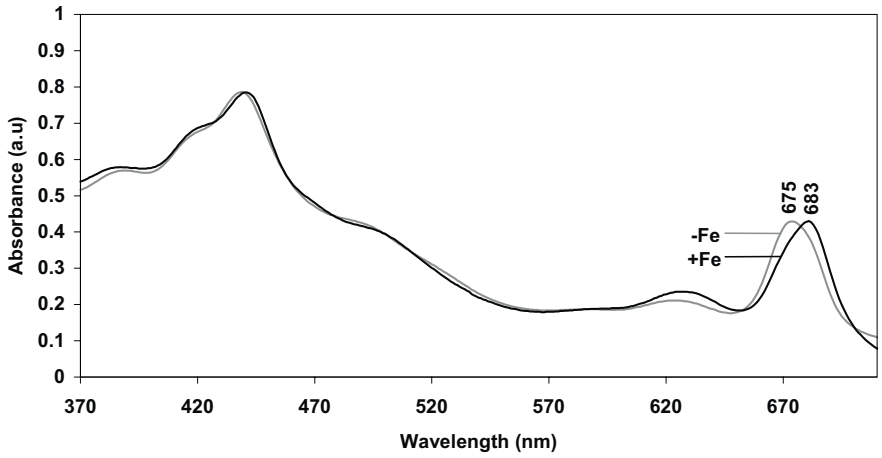

Fig. 1. Room temperature absorption spectra of thylakoid membranes isolated from the *cao* mutant of *Synechocystis* showing a characteristic blue shift in long-wavelength absorption maximum in response to iron deprivation. Thylakoid membranes were suspended in 50 mM MES pH 6.0, 0.5 M betaine, 5 mM $CaCl_2$, 5 mM $MgCl_2$ at 10 μM Chl.

column and the PSI fraction localised to the elutant. The PSI-enriched fraction was then layered on the top of a continuous sucrose gradient prepared according to the freeze–thaw method given in Hankamer et al. [14]. For the *cao*-plus mutant no prior separation of PSII and PSI was made and the supernatant obtained after DM treatment and centrifugation was layered onto the same continuous sucrose gradients. Both were subjected to 12 h of centrifugation at 26 000 rpm using a Beckman SW28 rotor.

2.2. Biochemical characterisation

Sodium dodecyl sulphate–polyacrylamide gel electrophoresis (SDS–PAGE) was performed as reported previously [12]. Optical absorption spectra were measured at room temperature using a Shimadzu MPS 2000 spectrometer. Steady-state fluorescence spectra were obtained using a Perkin Elmer LS50 at 77 K and measured with an excitation wavelength of 440 nm. Fluorescence excitation spectra were measured over the appropriate spectral ranges for the emission being detected at 77 K. Pigments were extracted into acetone and after recording their absorption and emission spectra, subjected to quantitative high pressure liquid chromatography (HPLC) following the methodology given in Zheleva et al. [15].

2.3. Electron microscopy (EM) and image processing

Preparations were negatively stained with 2% uranyl acetate on glow-discharged carbon-evaporated grids and imaged using a Philips CM 100 electron microscope at 80 kV. The magnification was calibrated as being 51 500×. Eight electron micrographs were taken for each preparation and subsequently calculated to have the first minima of their contrast transfer functions to be in the range of 17–24 Å. Electron micrographs were digitised using a Leafscan 45 densitometer set at a step size of 10 μm. Single particle data sets were obtained by interactively selecting all possible particles from the micrographs. All subsequent processing was performed within the IMAGIC-5 software environment [16,17]. The single particle images were coarsened by a factor of 2 resulting in a sampling frequency of 3.88 Å per pixel on the specimen scale. Reference-free alignment coupled with multivariate statistical analysis [18] was used to classify each data set in order to identify initial class averages. These were then used for iterative refinement, resulting in the improved class averages.

2.4. Modelling

Co-ordinate data sets were obtained from the RCSB Data bank (www.rcsb.org) under the entry codes for 1JBO (PSI 2.5 Å structure [19] and 1FE1 (PSII 3.8 Å structure) [20]. These structural models were visualised using the program Swiss-PDB viewer (Glaxo-Wellcome Experimental Research) [21] and overlaid at the same scale onto the calculated single particle projection maps. The carbon-α backbone for the transmembrane helices of the CP43 subunit was extracted from the 1FE1 co-ordinates and modeled into each subunit of the ring surrounding the PSI trimer, according to the centre of mass observed for each of the 18 subunits within the ring.

3. Results

Thylakoid membranes were isolated from the *cao*-plus mutant grown in the presence of iron and in iron-deficient media. Fig. 1 shows the absorption spectra of the isolated membranes where it can be seen that iron deprivation induces a blue shift of the far-red absorption maximum by 8 nm similar to that reported previously for the wild type [12,13]. There are, however, no obvious absorption features indicative of the presence of Chl *b* in either spectrum. In order to check whether Chl *b* had been synthesised in the *cao*-plus mutant, Chl was extracted and subjected to HPLC analysis. Fig. 2a shows the

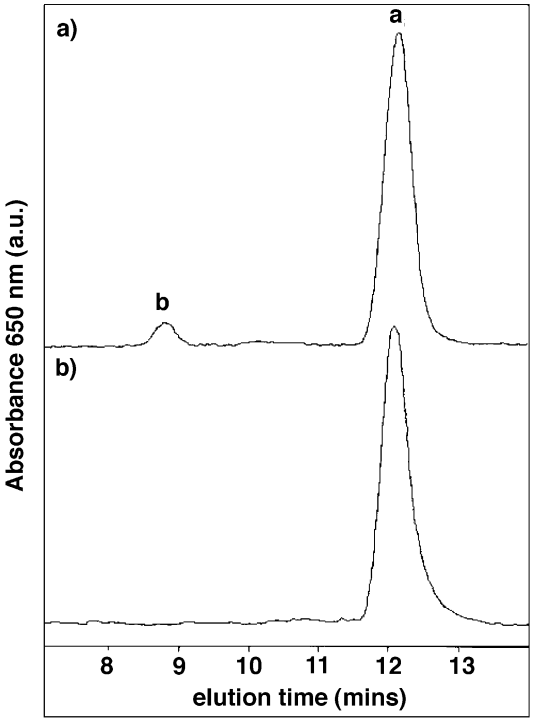

Fig. 2. HPLC elution profiles of Chl extracted from thylakoid membranes of cells of (a) the *cao* mutant and (b) the mutant of *Synechocystis* with His-tagged Chl-binding proteins grown in the presence of iron.

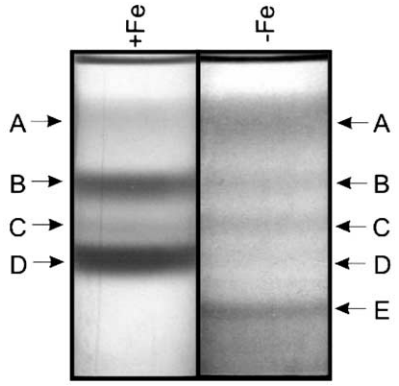

Fig. 3. Sucrose density-banding profile of products derived from DM solubilisation of isolated thylakoids from cells of the *cao* mutant grown in the presence (+Fe) or absence of iron (−Fe). +Fe: A = carotenoid, B = PSI/PSII monomers, C = PSII dimers, D = PSI trimers. −Fe: A = carotenoid/CP43′, B = PSI/PSII monomers, C = PSII dimers, D = PSI trimers, E = CP43′-PSI supercomplex.

HPLC trace of the Chl extracted from thylakoid membranes of *cao*-plus mutant grown in the presence of iron. Using Chl *a* and Chl *b* standards it was shown that the smaller peak corresponds to Chl *b* and the larger to Chl *a*. This was confirmed by conducting a similar analysis on the thylakoid membranes of *Synechocystis* cells with a His tag attached to the carboxy-terminus of the PSII Chl *a*-binding protein, CP47 [13]. These cells contained only Chl *a* (Fig. 2b). Calibrations with the Chl *a* and Chl *b* standards indicated that the Chl *b* level varied between different cultures and ranged from about 4 to 7% of the total Chl. A similar level was detected in thylakoid membranes isolated from *cao*-plus cells grown under iron-free conditions. Slightly higher amounts of Chl *b* could accumulate under iron-rich conditions, but as reported previously [10] the level was dependent on the growth rate of the culture, which in the case of the iron-free condition was less vigorous.

In order to explore whether Chl *b* was located in the CP43′ protein and therefore in the CP43′-PSI supercomplex reported previously [12,13], we solubilised the membranes with DM and separated the resulting complexes by sucrose density gradient centrifugation. Fig. 3 shows the profiles obtained with the *cao*-plus mutant. The cells grown in the presence of iron gave four bands, A, B, C and D, while the minus-iron condition induced an additional heavy band, E. Inspection of these bands by absorption and emission spectroscopy, SDS–PAGE and EM indicated that band A from the plus-iron cells consisted of free carotenoid while the corresponding band in the minus-iron cells contained CP43′ as well as free carotenoids. In both cases band B contained PSII and PSI complexes in their monomeric states. Band C was mainly PSII

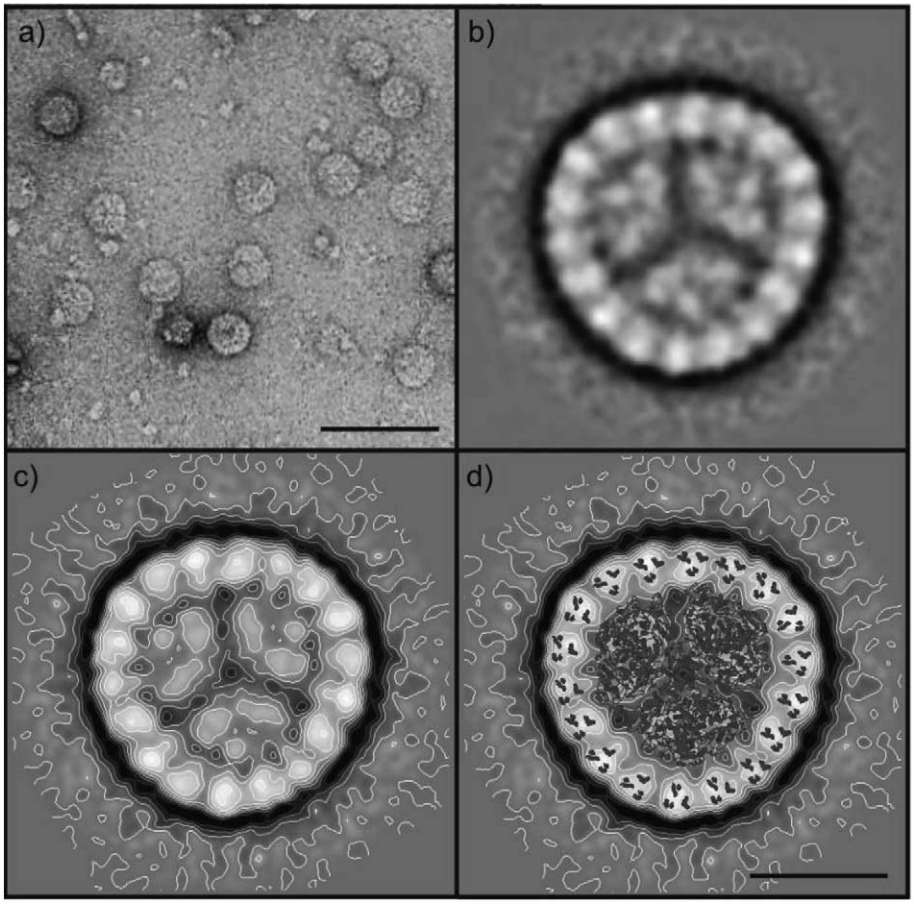

Fig. 4. Electron micrograph and projection maps and modeling of the CP43′-PSI supercomplex of the *cao* mutant of *Synechocystis*. a: Typical electron micrograph showing images of the top view of negatively stained CP43′-PSI supercomplex as a circular particle of approximately 330 Å in diameter (bar = 1000 Å). b: Projection map derived from averaging 3576 particles and image processing viewed from the stromal surface. c: Same as b but in contour presentation. d: Overlay of X-ray C_α structures of the PSI trimer [19] and of the six transmembrane helices of CP43 [20] (bar = 150 Å).

Table 1
Chl *b* levels in *cao* mutant of *Synechocystis* grown in minus-iron culture medium

Photosynthetic fraction	Chl *b* (%)
Thylakoids from iron-deficient cells	3.6
CP43′-PSI supercomplex	3.7
Free CP43′ dissociated from the CP43′-PSI supercomplex	3.6
PSI trimers dissociated from the CP43′-PSI supercomplex	3.6

dimers while band D, which was significantly reduced in the iron-depleted cells compared to normal cells, contained mainly PSI trimers. Band E, observed only when the cells were grown in minus-iron medium, consisted almost entirely of the CP43′-PSI supercomplex. Images of this complex are shown in Fig. 4a and the averaged top views shown in Fig. 4b. The latter is also shown in Fig. 4c as a contour map with the overlay of X-ray data in Fig. 4d. It can be seen that the 2.5 Å X-ray structure of the PSI trimer of *Synechococcus elongatus* determined by Jordan et al. [19] is accommodated in the central region of the projection map. Similarly, the overlaying of the transmembrane helices of CP43, obtained by X-ray diffraction [20], is consistent with the presence of 18 copies of the CP43′ protein in the ring surrounding the PSI reaction centre trimer. At the resolution of the projection map it seems that this CP43′-PSI supercomplex is identical to that isolated previously from *Synechocystis* with a His tag [12,13] and from wild type *Synechococcus* [22]. The absorption and fluorescence properties were also comparable with those reported previously [12,13] indicating that the CP43′ antenna was functionally associated with the reaction centre.

To determine whether Chl *b* in the supercomplex was present, HPLC was conducted following the same procedure as for thylakoid membranes. In this particular experiment the percentage of Chl *b* compared to the total Chl was in the region of 3.7 for the CP43′-PSI supercomplex, comparable with the level determined for the thylakoids from which they were isolated (Table 1). Using mild DM treatment the isolated supercomplexes were dissociated into their components, CP43′ and PSI trimers, followed by pigment analyses. As Table 1 shows, the percentage of Chl *b* remained constant in CP43′ and the PSI trimer.

4. Discussion

The formation of the 18-mer CP43′ subunit antenna ring around the PSI reaction centre trimer is probably a strategy to compensate for the reduction in the levels of phycobiliproteins and a decrease in the PSI/PSII ratio under iron-limiting conditions [8]. Normally CP43′ contains only Chl *a*, and based on the recent X-ray analyses of CP43 [23] there are probably 13 molecules bound to each copy of the protein. Therefore the 234 Chl *a* molecules contained in the 18-mer CP43′ antenna ring increase the light-harvesting capacity of PSI by 81%, given that the trimer binds 288 Chl *a* molecules, according to the recently determined X-ray structure of PSI [19]. Here we show that the *cao*-plus mutant also forms the 18-mer CP43′ antenna ring under iron stress conditions but in this case contains Chl *b* as well as Chl *a*. The level of Chl *b* is, however, relatively low and was found to be dependent on the stage of growth of the culture as previously noted [10]. Higher levels of Chl *b* have been obtained in a PSI-less *cao*-plus mutant when the *lhcb* gene of pea was also engineered into *Synechocystis* along with the *Arabidopsis cao* gene [11].

The binding of Chl *b* as well as Chl *a* to CP43′ in the *cao*-plus *Synechocystis* mutant is of interest because of the similarity of CP43′ to the Chl *a*/Chl *b* Pcb-binding proteins of prochlorophytes [7] in which an 18-mer Pcb antenna ring has been detected [24]. The level of Chl *b* can also be relatively low (6–20%) [25–27] in prochlorophytes, such as *Prochloron didemni*, *Prochlorothrix hollandica* and certain strains of *Prochlorooccus marinus*, like MED4. However, in the low light-adapted *Prochlorococcus* strain SS120 the Chl *b* level can be as high as 66%, which is more comparable with the levels in some of the Cab proteins that act as light-harvesting systems for PSII [1]. Other Cab proteins, however, have significantly lower levels of Chl *b* [1] and the factors which control the different levels of Chl *b* in light-harvesting proteins are unknown. The *cao*-plus cyanobacterial mutant used here offers an in vivo experimental system to investigate these differences.

References

[1] Green, B.R. and Durnfold, D.G. (1996) Annu. Rev. Plant Physiol. Plant Mol. Biol. 47, 685–714.
[2] Margulis, L. (1981) Symbiosis in Cell Evolution, Freeman, San Francisco, CA.
[3] Bhattacharya, D. and Medlin, L. (1998) Plant Physiol. 116, 9–15.
[4] Sidler, W. (1994) in: Molecular Biology of Cyanobacteria (Bryant, D.A., Ed.), pp. 139–216, Kluwer Academic, Dordrecht.
[5] Lewin, R.A. (1976) Nature 261, 697–698.
[6] Partensky, F., Hess, W.R. and Vaulot, D. (1999) Microbiol. Mol. Biol. Rev. 63, 106–127.
[7] La Roche, J., van der Staay, G.W., Partensky, F., Ducret, A., Aebersold, R., Li, R., Golden, S.S., Hiller, R.G., Wrench, P.M. and Larkum, A.W. (1996) Proc. Natl. Acad. Sci. USA 93, 15244–15248.
[8] Strauss, N.A. (1994) in: Molecular Biology of Cyanobacteria (Bryant, D.A., Ed.), pp. 731–750, Kluwer Academic, Dordrecht.
[9] Oster, U., Tanaka, R., Tanaka, A. and Rudiger, W. (2000) Plant J. 21, 305–310.
[10] Satoh, S., Ikeuchi, M., Mimuro, M. and Tanaka, A. (2001) J. Biol. Chem. 276, 4293–4297.
[11] Xu, H., Vavilin, D. and Vermaas, W. (2001) Proc. Natl. Acad. Sci. USA 98, 14168–14173.
[12] Bibby, T.S., Nield, J. and Barber, J. (2001) J. Biol. Chem. 276, 43246–43252.
[13] Bibby, T.S., Nield, J. and Barber, J. (2001) Nature 412, 743–745.
[14] Hankamer, B., Nield, J., Zheleva, D., Boekema, E.J., Jansson, S. and Barber, J. (1997) Eur. J. Biochem. 243, 422–429.
[15] Zheleva, D., Hankamer, B. and Barber, J. (1996) Biochemistry 35, 15074–15079.
[16] van Heel, M., Harauz, G. and Orlova, E.V. (1996) J. Struct. Biol. 116, 17–24.
[17] van Heel, M., Gowen, B., Matedeen, R., Orlova, E.V., Finn, R., Pape, T., Cohen, D., Stark, H., Schmidt, R., Schatz, M. and Patwardhan, A. (2000) Q. Rev. Biophys. 33, 307–369.
[18] Sherman, M., Soejima, T., Chui, W. and van Heel, M. (1998) Ultramicroscopy 74, 179–199.
[19] Jordan, P., Fromme, P., Witt, H.T., Klukas, O., Saenger, W. and Kraus, N. (2001) Nature 411, 909–916.

[20] Zouni, A., Witt, H.T., Kern, J., Fromme, P., Krauss, N., Saenger, W. and Orth, P. (2001) Nature 409, 739–743.
[21] Guex, N. and Peitsch, M.C. (1997) Electrophoresis 18, 2714–2723.
[22] Boekema, E.J., Hiffney, A., Yakushevska, A.E., Piotrowski, M., Keegstra, W., Berry, S., Michel, K.-P., Pistorius, E.K. and Kruip, J. (2001) Nature 412, 745–748.
[23] Kamiya, N. and Shen, J.R. (2003) Proc. Natl. Acad. Sci. USA 100, 98–102.
[24] Bibby, T.S., Nield, J., Partensky, F. and Barber, J. (2001) Nature 413, 590.
[25] Matthijs, H.C.P., van der Staay, G.W.M., van Amerongen, H., van Grondelle, R. and Garab, G. (1989) Biochim. Biophys. Acta 975, 185–187.
[26] Lewin, R.A. and Withers, N.W. (1975) Nature 256, 735–737.
[27] Garczarek, L., van der Staay, G.W.M., Thomas, J.C. and Partensky, F. (1998) Photosynth. Res. 56, 131–141.